JACS
JOURNAL OF THE AMERICAN CHEMICAL SOCIETY
Article
pubs.acs.org/JACS

A Gold Exchange: A Mechanistic Study of a Reversible, Formal Ethylene Insertion into a Gold(III)−Oxygen Bond

Eirin Langseth,[†] Ainara Nova,*[,‡] Eline Aa. Tråseth,[†] Frode Rise,[†] Sigurd Øien,[†] Richard H. Heyn,[§] and Mats Tilset*[,†,‡]

[†]Department of Chemistry and [‡]Centre for Theoretical and Computational Chemistry (CTCC) Department of Chemistry, University of Oslo, P.O. Box 1033, Blindern, N-0315 Oslo, Norway

[§]SINTEF Materials and Chemistry, P.O. Box 124, Blindern, N-0314 Oslo, Norway

Supporting Information

ABSTRACT: The Au(III) complex $Au(OAc^F)_2(tpy)$ (**1**, OAc^F = $OCOCF_3$; tpy = 2-*p*-tolylpyridine) undergoes reversible dissociation of the OAc^F ligand *trans* to C, as seen by ^{19}F NMR. In dichloromethane or trifluoroacetic acid (TFA), the reaction between **1** and ethylene produces $Au(OAc^F)(CH_2CH_2OAc^F)(tpy)$ (**2**). The reaction is a formal insertion of the olefin into the Au−O bond *trans* to N. In TFA this reaction occurs in less than 5 min at ambient temperature, while 1 day is required in dichloromethane. In trifluoroethanol (TFE), $Au(OAc^F)(CH_2CH_2OCH_2CF_3)(tpy)$ (**3**) is formed as the major product. Both **2** and **3** have been characterized by X-ray crystallography. In TFA/TFE mixtures, **2** and **3** are in equilibrium with a slight thermodynamic preference for **2** over **3**. Exposure of **2** to ethylene-d_4 in TFA caused exchange of ethylene-d_4 for ethylene at room temperature. The reaction of **1** with *cis*-1,2-dideuterioethylene furnished $Au(OAc^F)$(*threo*-$CHDCHDOAc^F$)(tpy), consistent with an overall *anti* addition to ethylene. DFT(PBE0-D3) calculations indicate that the first step of the formal insertion is an associative substitution of the OAc^F *trans* to N by ethylene. Addition of free $^-OAc^F$ to coordinated ethylene furnishes **2**. While substitution of OAc^F by ethylene *trans* to C has a lower barrier, the kinetic and thermodynamic preference of **2** over the isomer with $CH_2CH_2OAc^F$ *trans* to C accounts for the selective formation of **2**. The DFT calculations suggest that the higher reaction rates observed in TFA and TFE compared with CH_2Cl_2 arise from stabilization of the $^-OAc^F$ anion lost during the first reaction step.

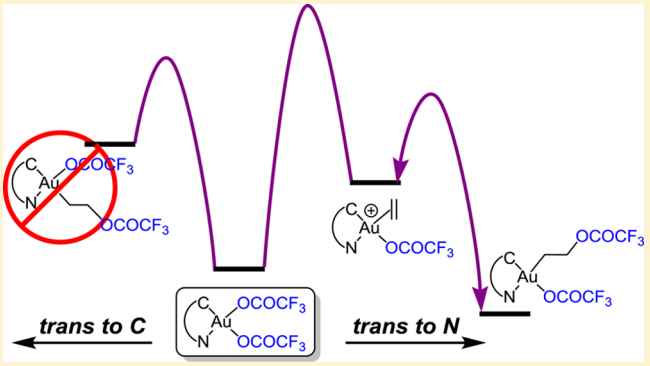

INTRODUCTION

There has been a growing interest in gold chemistry during the last two decades.[1,2] Gold complexes catalyze a variety of organic transformations, including aldol reactions, benzannulations, and additions of nucleophiles to C−C multiple bonds.[3−13] Although Au(I) is still used most frequently in catalysis, Au(III) complexes are currently rising to prominence and finding new applications as catalysts.[14] It is of considerable practical interest that Au(III) complexes are usually quite tolerant toward water and oxygen, which facilitates their use as catalysts under ambient conditions.[3] In addition, the participation of Au(III) complexes as catalysts or intermediates in oxidative catalytic reactions[15−19] has triggered the growing interest in understanding and developing further the reactivity of such complexes.

Although homogeneous gold catalysis is an active and maturing field, a better understanding of reaction mechanisms is still desired. Computational methods have been successfully used to shed light on and supplement experimental data for the preferred mechanisms of several reactions.[20−25] Experimental efforts have been dedicated to the isolation or observation of key intermediates[26−29] and elementary steps[30−37] that are suggested by either experiments or computations.[38,39] It is worth noting that an Au(III) hydride[27] as well as several Au(III) vinyl complexes have been isolated recently. By analogy to the chemistry of Au(I), Au(III) π-complexes are assumed to be key intermediates in the catalytic functionalization of olefins,[28,29] as these may be functionalized by the addition of nucleophiles.[40] Au(III) complexes with π-bonded ligands, such as alkenes, allenes, alkynes, and CO, have, however, rarely been observed,[28] and it was only very recently that the first unambiguously characterized Au(III) alkene complexes were reported. Bochmann and co-workers[41] successfully prepared a series of Au(III) alkene complexes bearing the C^N^C pincer ligand depicted in Scheme 1a, and our group[42] reported the first X-ray structure of a Au(III) alkene complex, [Au(cod)-Me_2][BArf] (cod =1,5-cyclooctadiene; BArf = B(3,5-$C_6H_3(CF_3)_2)_4$). There are so far no examples of isolated Au(III) complexes of alkynes, allenes, or CO.

The functionalization of alkenes has great practical value.[40] There are, however, only a handful of examples of the

Received: May 9, 2014
Published: June 19, 2014

   dx.doi.org/10.1021/ja504554u | J. Am. Chem. Soc. 2014, 136, 10104−10115

Scheme 1. Formal Insertion of Ethylene into Au−OAc^F Bonds:[a] (a) Bochmann's Reported Pincer Complex A; (b) Reaction of Au(OAc^F)$_2$(tpy) (1) with Ethylene in TFA To Form 2

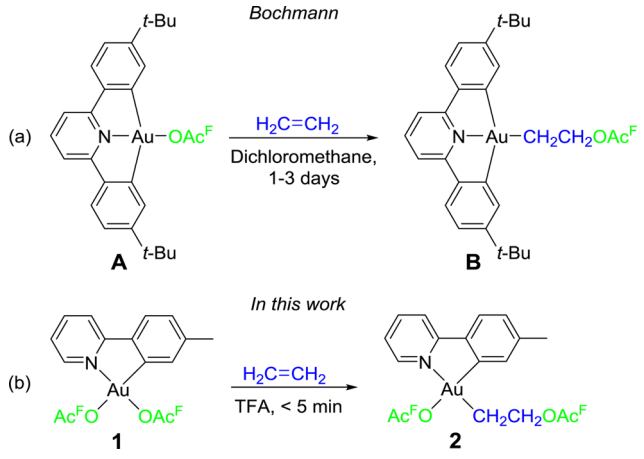

[a]TFA = CF_3COOH.

functionalization of alkenes with Au(III) and no mechanistic studies of the reactions. This contrasts with the detailed mechanistic insight that is established for the well-known Pd-catalyzed Wacker oxidation of ethylene.[43,44] Atwood and co-workers recently reported that ethylene and propylene could be stoichiometrically functionalized with Au(III) complexes in water.[45] The group of Bochmann showed that ethylene slowly inserts into the Au(III)−OAc^F (OAc^F = $OCOCF_3$) bond in **A** in dichloromethane; see Scheme 1a.[41]

In this paper, we report details of the reactivity of Au(OAc^F)$_2$(tpy) (**1**, tpy =2-*p*-tolylpyridine) with ethylene. Formal ethylene insertion occurs selectively into one of the two available Au−OAc^F bonds. Interestingly, the insertion occurs at the position that is *trans* to the *weakest trans* effect atom (N) of the tpy N−C chelate (Scheme 1b). Whereas the reaction proceeds slowly in dichloromethane, with rates comparable to those reported in the same solvent by Bochmann and co-workers (1−3 days),[41] we find a remarkable acceleration of the reaction in the protic solvents trifluoroacetic acid (TFA) and trifluoroethanol (TFE); the insertion is observed within minutes in TFA-*d* (Scheme 1). The mechanistic details of this reaction have been investigated experimentally and computationally and provide a consistent description of the system. Our findings, which bear relevance to Au-mediated stoichiometric and catalytic functionalization of alkenes, reveal that ethylene binding as well as attack by nucleophiles at the coordinated ethylene ligand are reversible processes.

RESULTS AND DISCUSSION

The starting Au(III) complex for this investigation, Au(OAc^F)$_2$(tpy) (**1**),[46] can be readily synthesized in good yields by the use of microwave heating from either Au(OAc)$_3$ (as previously reported) or from the less expensive Au(OH)$_3$. Complex **1** provides easy access to a range of cyclometalated Au(III) mono- or dialkyl species via reactions with Grignard or organolithium reagents.[46]

The solution behavior of **1** as seen by ^{19}F NMR bears direct relevance to the reaction chemistry. In the poorly coordinating solvents dichloromethane-d_2 and benzene-d_6, two quite sharp singlets are observed (half-height peak widths ω = 4.3 and 4.7 Hz in benzene-d_6; 3.5 and 4.0 Hz in dichloromethane-d_2), as expected for the CF_3 groups of the nonequivalent OAc^F ligands. These were unambiguously assigned by a ^{19}F−^{1}H HOESY experiment.[46] However, in acetonitrile-d_3 the signal at the lower ppm value, arising from the CF_3 group *trans* to the C of the tpy chelate, is considerably broadened (ω = 90 Hz).[47] A lowering of the temperature from ambient to 10 °C causes this signal to sharpen to 37 Hz. In acetic acid-d_4, the signal is even broader (ω = 281 Hz). The signal at the higher ppm value, caused by CF_3 *trans* to N, remains sharp with ω = 2.1 Hz in acetonitrile-d_3 and 4.3 Hz acetic acid-d_4 (spectra are shown in the Supporting Information). When NaOAc^F is added to a solution of Au(OAc^F)$_2$(tpy) in acetonitrile-d_3, two signals are still seen in the ^{19}F NMR spectrum. The signal corresponding to the CF_3 group *trans* to N remains sharp. Free $^-$OAc^F and the OAc^F ligand *trans* to C give rise to one broadened signal. This signal appears at a chemical shift that is slightly dependent on the amount of NaOAc^F added, but the ppm value is always between that of the coordinated OAc^F groups (at −74.8 and −75.6 ppm in the absence of added NaOAc^F) and that of pure NaOAc^F in acetonitrile-d_3 (−76.6 ppm).

A further investigation of the dependence of the signal broadening on temperature, solvent, or concentrations has not been undertaken, as the conclusions to be drawn are quite clear. The pronounced broadening that is seen in polar solvents suggests that the OAc^F ligand *trans* to C (the part of the N−C chelate ligand that has the strongest *trans* effect) undergoes fast and reversible dissociation in solution. The broadening is caused by exchange of bonded OAc^F and free $^-$OAc^F anion. This is further supported by a ^{19}F−^{19}F NOESY spectrum obtained for **1** (Figure 1). The spectrum, recorded in acetonitrile-d_3, shows two expected cross peaks, which confirms that the two CF_3 groups are indeed in close proximity in space as they are both bonded to the Au center. A complete dissociation of the OAc^F ligand to form an ionic species can be ruled out, since a free $^-$OAc^F anion would not show the NOESY interaction with the OAc^F that remains bonded at gold. There are a few reported examples of ^{19}F−^{19}F NOESY spectra in the literature,[48−53] including an Ru organometallic system,[48] and multidimensional fluorine NMR applications have been reviewed.[54]

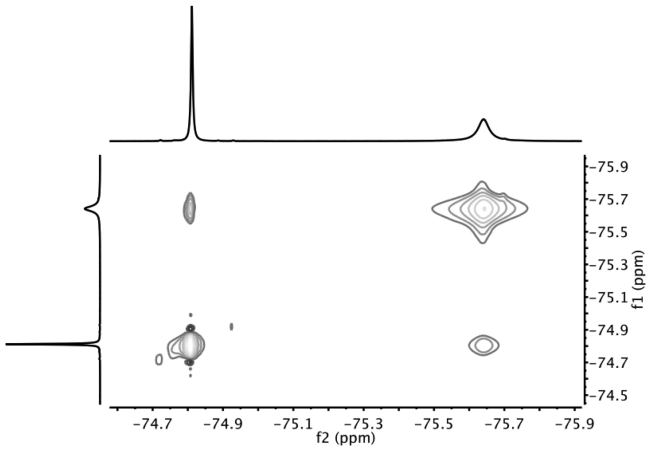

Figure 1. ^{19}F−^{19}F NOESY spectrum of Au(OAc^F)$_2$(tpy) (**1**).[55] The broad signal corresponds to the CF_3 group *trans* to the C of the N−C chelate.

dx.doi.org/10.1021/ja504554u | J. Am. Chem. Soc. 2014, 136, 10104−10115

Scheme 2. Formal Insertion of Ethylene To Form 2 and 3 in TFA and TFE, Respectively

Reactivity of $Au(OAc^F)_2(tpy)$ with Ethylene. When ethylene was bubbled through a solution of **1** in trifluoroacetic acid-*d* at room temperature, an almost immediate color change from light yellow to colorless was observed. The only product seen by ^1H NMR was $Au(OAc^F)(CH_2CH_2OAc^F)(tpy)$, **2** (Scheme 2), arising from a formal insertion of ethylene into the Au−O bond *trans* to N. It is particularly intriguing that the formal insertion has occurred at the coordination site of the OAc^F ligand that is *trans* to N (weakest *trans* effect), whereas the one-dimensional ^{19}F and $^{19}F-^{19}F$ NOESY NMR showed that OAc^F ligand dissociation occurs at the site *trans* to C (strongest *trans* effect). This issue will be further addressed in the discussion of DFT calculations, which helps to provide a comprehensive view of the reaction mechanism (vide infra). When the reaction is followed by ^1H NMR in TFA-*d*, full conversion of **1** to **2** is complete within less than 5 min, as seen from the appearance of two new triplets at 4.79 and 2.40 ppm with $^3J_{HH}$ = 7.9 Hz for the two new methylene groups arising from inserted ethylene. The reaction was essentially quantitative by NMR, and complex **2** was isolated in 76% yield. Interestingly, reaction of Bochmann's C^N^C pincer complex **A**[41] (Scheme 1a) in the presence of protic species led to protolysis of one Au−C chelate bond. No hint of such behavior was seen for **1**, even in a medium as acidic as TFA. The difference between the two systems may be attributed to a greater ring strain in the doubly chelated system in **A**. Note also that there is no regiochemical issue for the formal insertion in Bochmann's system which contains only one OAc^F ligand, positioned *trans* to the chelate N atom.

The reaction between **1** and ethylene in trifluoroethanol (TFE) yields $Au(OAc^F)(CH_2CH_2OCH_2CF_3)(tpy)$ (**3**) as the major product, instead of **2** (Scheme 2). When this reaction is performed in TFE-d_3 and monitored by ^1H NMR, it is seen that the conversion to **3-d_2** is completed in ca. 30 min, as seen from the appearance of two new triplets at 3.97 and 2.26 ppm with $^3J_{HH}$ = 7.8 Hz for the methylene protons derived from the inserted ethylene (the methylene unit from TFE-d_3 is of course ^1H NMR silent). The reaction to form **3-d_2** in TFE-d_3 is considerably slower than the reaction to form **2** in TFA-*d*. Monitoring of the reactions between **1** and ethylene to furnish **2** and **3-d_2** by ^1H NMR spectroscopy is very convenient, as the singlet for the aryl−H *ortho* to Au and Me in the tolyl group, the aromatic signal at the lowest chemical shift, moves significantly to a higher ppm value upon reaction ($\Delta\delta$ between 0.65 and 0.31 ppm depending on complex and solvent) when **1** is converted to **2** or **3-d_2**. In situ NMR analysis showed essentially quantitative yield of **3-d_2** in TFE-d_3; traces of **2** were detectable, estimated at <0.5%. When **3** was isolated on a larger scale, **2** was always present in the isolated product, ca. 5% of the reaction mixture. These results suggests that, in addition to the occurrence of the initial formal insertion of ethylene into an Au−OAc^F bond, external nucleophilic addition of a solvent molecule (TFA or TFE) to a putative, unobserved Au−ethylene intermediate complex is feasible. A related reaction was observed when Bochmann's complex **A** (Scheme 1a) was treated with norbornene and methanol. However, protolysis of one chelated Au−C bond accompanied this reaction.[41]

The choice of solvent for the reaction between **1** and ethylene has a strong influence on the reaction rate, not only on the identity of the product (**2** vs **3**). In the poorly coordinating and less polar solvent dichloromethane-d_2, only 40% conversion of **1** to **2** was seen after 2 h at room temperature, compared with full conversion in less than 5 min in TFA-*d*. After 24 h, the yield from the reaction in dichloromethane-d_2 was ca. 94% (^1H NMR, internal standard). Thus, in a qualitative sense, the reaction rate increases with increasing solvent polarity and with hydrogen bonding ability.

The new complexes **2** and **3** are stable in dichloromethane-d_2 solution over the course of several weeks (as monitored by ^1H NMR). In TFA-*d*, the stability of **2** is somewhat diminished, with some observable decomposition of **2** within a day. Approximately 25% of **2** had decomposed to unidentified products over the course of 5 days. The complexes **2** and **3** were further characterized by ^{13}C and ^{19}F NMR spectroscopy and mass spectroscopy.

The reaction comes to a stop after one formal ethylene insertion. Catalysis of neither ethylene polymerization nor addition of $HOAc^F$ to ethylene was observed. Attempts to make the latter reaction catalytic were performed by monitoring the reaction in TFA-*d* at elevated pressures (60 atm ethylene, 50 °C),[56] or by adding the stronger triflic acid to the medium in order to facilitate a protolytic cleavage of the Au−alkyl bond in the insertion product **2** (which would complete a catalytic cycle). The apparent difficulty with protolysis of the Au−alkyl bond in **2** agrees with our previous finding that treatment of $Au(tpy)Me_2$ leads to initial protolytic cleavage of the *chelate* Au−C(sp^2) bond rather than of an Au−Me(sp^3) bond.[42]

Crystallographic Structure Determination of the Au(III) Complexes 2 and 3. The structures of **2** and **3** were determined by single-crystal X-ray diffraction analysis. ORTEP plots of the structures are shown in Figures 2 and 3, respectively. Crystallographic data and metric parameters are given in the Supporting Information. The two complexes exhibit square planar coordination geometry, as expected for Au(III) complexes, and show quite similar solid-state structures. The Au−N bond distances are approximately 0.1 Å greater in **2** and **3** than in **1**.[46] This is likely due to the stronger *trans* influence of the alkyl ligands in **2** and **3** compared to the OAc^F ligand in **1**. The alkyl ligands formed from ethylene insertions are *trans* to a pyridine N and have rather similar Au−C distances at 2.042(3), 2.040(4), and 2.055(11) Å in **2**, **3**, and **B**,[41] respectively. The Au−O bond distances to the OAc^F ligand *trans* to C are quite similar, 2.111(5), 2.104(2), and 2.110(3) Å, for **1**, **2**, and **3**, respectively. The bond angles around the Au central atom are fairly similar in the three complexes **1**, **2**, and **3**, with no differences greater than 4.3° for corresponding angles. The chelate angles are normal for such cyclometalated species at 81.8(3)°, 81.80(11)°, and 81.48(17)° for **1**, **2**, and **3**, respectively. The bond angles described by the two non-

dx.doi.org/10.1021/ja504554u | J. Am. Chem. Soc. 2014, 136, 10104−10115

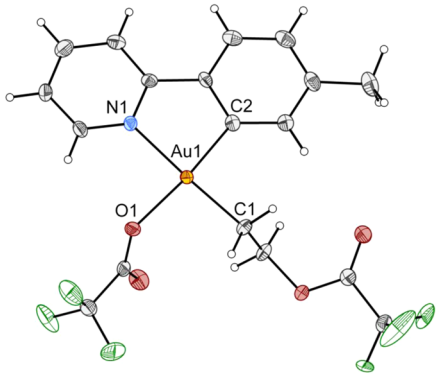

Figure 2. ORTEP view of the solid-state structure of **2** (100 K) with 50% probability displacement ellipsoids. Selected bond distances (Å) and angles (deg): Au1−C1, 2.042(3); Au1−C2, 1.993(3); Au1−N1, 2.098(2); Au1−O1, 2.104(2); C1−Au1−C2, 95.12(12); C1−Au1−N1, 176.80(11); C1−Au1−O1, 90.20(10); C2−Au1−N1, 81.80(11); C2−Au1−O1, 174.42(10); N1−Au1−O1, 92.90(9). The CF_3 group on the ligand where ethylene inserted was disordered with a 1:1 population of the two orientations, of which only one is shown.

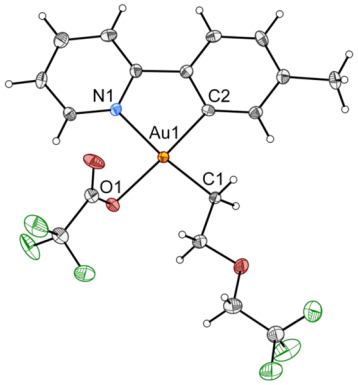

Figure 3. ORTEP view of the solid-state structure of **3** (100 K) with 50% probability displacement ellipsoids. Selected bond distances (Å) and angles (deg): Au1−C1, 2.040(4); Au1−C2, 2.006(4); Au1−N1, 2.107(4); Au1−O1, 2.110(3); C1−Au1−C2, 92.09 (18); C1−Au1−N1, 173.52(16); C2−Au1−N1, 81.48(17); C1−Au1−O1, 91.77(16); C2−Au1−O1, 175.61(16); N1−Au1−O1, 94.68(14).

chelating ligands are close to 90° (O−Au−O 88.8(2)° for **1**, C−Au−O 90.20(10)° for **2**, and C−Au−O 91.77(16)° for **3**). The dominating intermolecular interactions that are discernible for the packing in the crystal structures of **2** and **3** appear to be π-interactions. In **2**, there is a Au−π stacking (Au−tolyl distance of 3.570 Å). In **3** there is a pronounced π-stacking between the tolyl ring and the pyridine ring of a neighboring molecule, with a distance between the stacked aromatic rings of 3.697 Å. There appear to be no significant Au···Au interactions in the crystal structures of **2** and **3**, as the shortest intramolecular Au···Au distances are 4.826 and 4.831 Å, respectively.

Reversibility of the Reaction of 1 with Ethylene in TFA and TFE. The observation of **3**, rather than **2**, as the major product in the reaction between **1** and ethylene in TFE led us to consider whether the reaction might be reversible. Reversible amination of alkenes has been observed at Au(I).[57] It was postulated that the reversible step constituted an *anti* addition of amine to the alkene and that the subsequent protiodeauration was irreversible. Thus, the possible interconversion of **2** and **3** was explored in the appropriate solvents (Scheme 3).

Scheme 3. Interconversion between Complexes 2 and 3-d_2 in Solution

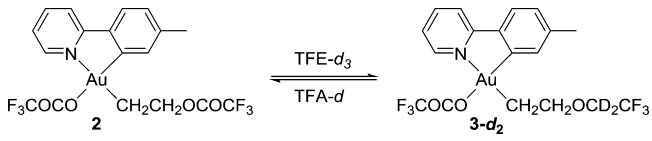

When isolated **3** was dissolved in TFA-*d* at room temperature, it reacted in less than 5 min to form only **2** (the reaction was completed before a ^{1}H NMR spectrum was acquired). Analogous behavior was observed for **2**; dissolution of **2** in TFE-d_3 converted it to **3-d_2**, but more slowly. Full conversion of **2** to **3-d_2** was achieved by overnight heating at 50 °C. In a solution of 1:1 (v/v) TFA-*d* and TFE-d_3, a **2**:**3-d_2** ratio of approximately 9:1 resulted after allowing the solution to equilibrate. The equilibrium was investigated further by ^{1}H NMR by varying the TFA-*d*/TFE-d_3 solvent composition. The spectra shown in Figure 4 are recorded after equilibrium was reached within a few hours. The ratio between **2** and **3-d_2** however changed only slightly from the first spectrum recorded after ethylene addition. At a given solvent composition, the relative **2** and **3-d_2** concentrations were determined by ^{1}H NMR and the equilibrium constant K_{eq} was calculated from eq 1. The measured K_{eq} data are given in the Supporting Information. Changes in the solvent composition from 90% TFA to 95% TFE caused a remarkably small variation of K_{eq}, and the average equilibrium constant for the interconversion of **2** to **3** in the entire solvent range was 0.18 ± 0.08, corresponding to a $\Delta G°$ difference of 1.1 ± 0.35 kcal/mol.[58] This indicates a slight thermodynamic preference for **2** over **3**.

$$K_{eq} = \frac{[\mathbf{3}][\mathrm{TFA}]}{[\mathbf{2}][\mathrm{TFE}]} \quad (1)$$

To further substantiate the conclusion that **2** was the thermodynamically preferred species between **2** and **3**, and to check if the preference also pertained to less polar and aprotic solvents, **1** was reacted with ethylene in dichloromethane-d_2 with 1.2 equiv of TFE present in the solution. Under these conditions, the cationic Au(III) moiety that results after a hypothetically complete OAc^F ligand dissociation was exposed to approximately equal concentrations of $^-OAc^F$ and TFE. Full conversion to **2** was seen within 1 day. There was no sign of complex **3** after 5 days, as confirmed by spiking the NMR sample with an authentic sample of **3**. This establishes that **2** is thermodynamically clearly preferred over **3** in this aprotic solvent.

The observed interconversion of **2** and **3** does not necessarily imply a complete reversibility of the reaction of **1** with ethylene in TFA or TFE. Rather, the observation is consistent with a reversible nucleophilic attack ($^-OAc^F$ or TFE) at coordinated ethylene, a behavior that is a common feature of such reactions,[40] and provides no information about the eventual reversibility of ethylene coordination. Therefore, a separate experiment was designed to probe for such reversibility. Thus, ethylene-d_4 was added to a solution of **1** in TFA-*d* at room temperature (see Scheme 4 and Figure 5). The expected signals for the insertion product **2-d_4** complex were observed in the ^{1}H NMR spectrum—characteristically without the two methylene group signals of **2**. Then unlabeled ethylene was bubbled through the solution of **2-d_4**. After approximately 5 min, the signals for the two methylene groups had appeared in the ^{1}H

dx.doi.org/10.1021/ja504554u | J. Am. Chem. Soc. 2014, 136, 10104−10115

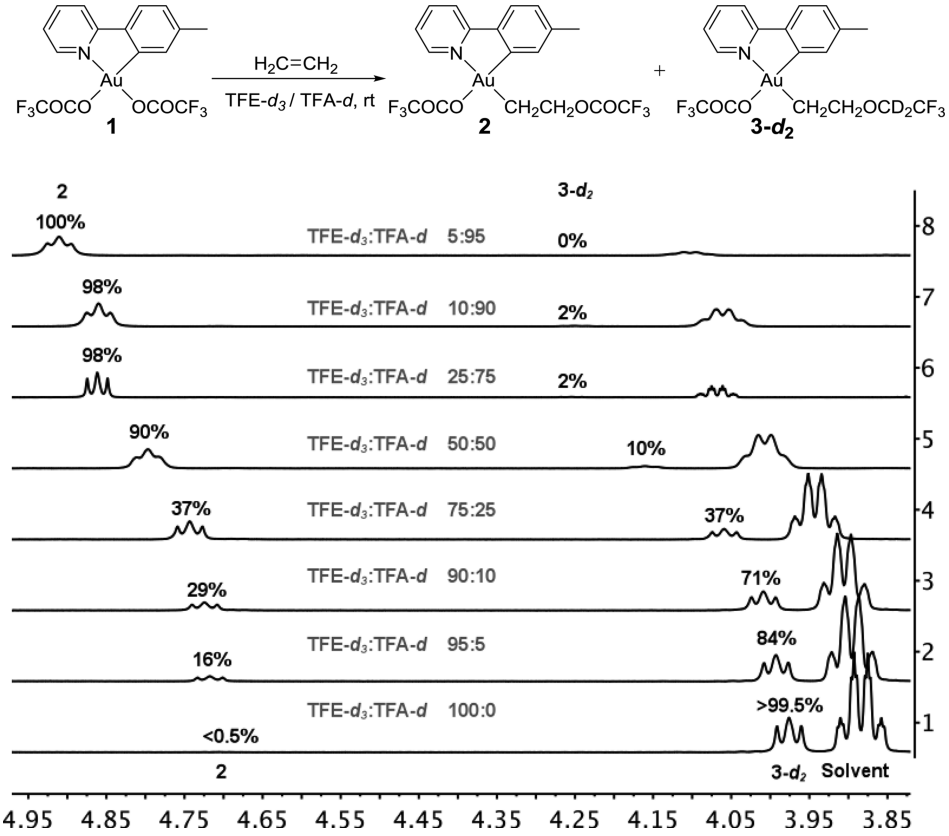

Figure 4. ^{1}H NMR (500 MHz, 25 °C) of **2** (left) and **3-d_2** (right) with varying solvent composition TFE-d_3/TFA-*d*. The solvent compositions (v/v) of TFE-d_3 and TFA-*d* are shown in the middle of the spectra. The signals shown arise from the OCH_2 groups in **2** and **3-d_2**. The large signal at ca. 3.9 ppm in the bottom spectrum (labeled "solvent") arises from residual protons in the TFE-d_3 of the solvent mixture. The chemical shifts of all protons are slightly solvent dependent. The full spectra are shown in the Supporting Information.

Scheme 4. Reversibility of the Ethylene Insertion

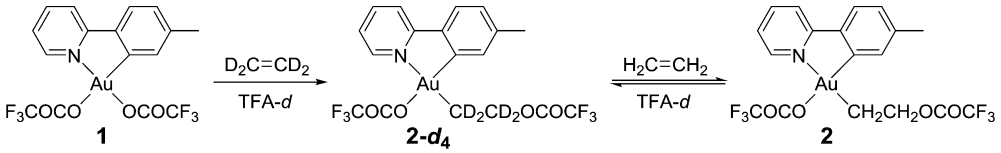

NMR spectrum (labeled with * in Figure 5), indicating a ca. 4:1 **2-d_4**:**2** ratio.

The experiment described above demonstrates that ethylene-d_4 and ethylene undergo exchange at Au. In principle, this might occur by a complete reversal of all steps back to **1**, or it might occur by an ethylene ligand-exchange process involving some other intermediate along the reaction pathway of the ethylene insertion. Attempts were made to probe whether the starting complex **1** could be accessed from preformed **2** by ethylene removal, either under vacuum or by purging a solution of **2** with inert gas. Several freeze–pump–thaw cycles on a solution of **2** in CD_2Cl_2 did not produce any observable quantities of **1**; neither did bubbling argon gas through a solution of **2** in TFA-*d*. However, when **2** was heated in TFA with slow Ar purge (50 °C, 1 h 15 min), detectable quantities of **1** were seen by ^{1}H NMR, along with considerable sample decomposition. This finding leaves the possibility open, but does not firmly prove, that **1** is involved in the ethylene/ethylene-d_4 exchange. This issue will be addressed when computational results are discussed later.

Nucleophilic Addition of $^-$OAc^F at 1: External or Internal Attack? Presuming ethylene coordination at Au by ligand substitution at **1**, an intermediate with the composition [Au(tpy)(OAc^F)(CH_2═CH_2)][OAc^F] may be generated. From this, the formation of the O–CH_2 bond may occur externally (intermolecularly), by attack of the dissociated $^-$OAc^F on coordinated ethylene,[39,59] or internally (intramolecularly), in which case the OAc^F ligand still coordinated at Au attacks the coordinated ethylene.[60] The former process will result in an *anti* addition of Au and O to ethylene, whereas the latter—which may be viewed as a type of direct insertion—results in a *syn* addition (Scheme 5). Although both inter- and intramolecular additions have been previously proposed, the intermolecular process has more experimental[61,62] and computational support.[57,59,63,64] The nature of the nucleophilic attack by water on coordinated ethylene has also been a key issue in mechanistic studies of the Wacker process.[44]

In order to establish whether the addition of OAc^F to coordinated ethylene occurs by an intermolecular or an intramolecular pathway, the reaction was conducted using *cis*-1,2-dideuterioethylene. Two diastereomers may result from the reaction between **1** and *cis*-1,2-dideuterioethylene, with the relative configurations *threo* (arising from an external, *anti*

dx.doi.org/10.1021/ja504554u | J. Am. Chem. Soc. 2014, 136, 10104–10115

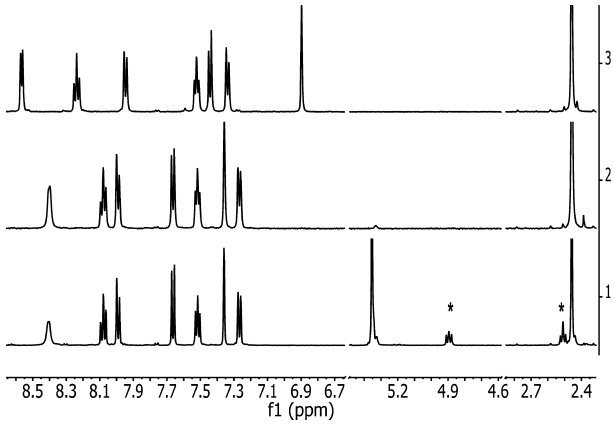

Figure 5. ^{1}H NMR (500 MHz, 25 °C, TFA-*d*) spectra showing the reversibility of the ethylene insertion. (Top) Spectrum of freshly dissolved Au(OAc^F)$_2$(tpy) (**1**). (Middle) After addition of $D_2C{=}CD_2$; spectrum shows **2-*d*$_4$**. (Bottom) After addition of $H_2C{=}CH_2$ to the deuterated complex **2-*d*$_4$** to give a mixture of **2-*d*$_4$** and **2**. The **2-*d*$_4$**:**2** ratio shown in the bottom spectrum is 4:1. Parts of the spectra have been omitted to improve the clarity. The full spectra are shown in the Supporting Information.

Scheme 5. Schematic Representation of the Inter- and Intramolecular Nucleophilic Additions of a $^-$OAc^F Anion or a OAc^F Ligand at Coordinated Ethylene

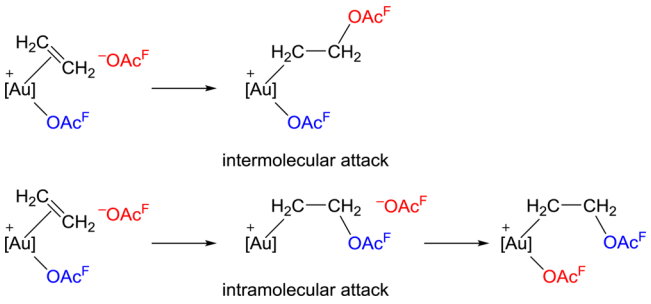

attack of $^-$OAc^F) and the *erythro* (internal, *syn* attack) at the two stereogenic centers that are produced (see Scheme 6).[65,66]

Scheme 6. *Threo* and *Erythro* Diastereomers of Au(OAc^F)(CHDCHDOAc^F)(tpy) (2-*d*$_2$)

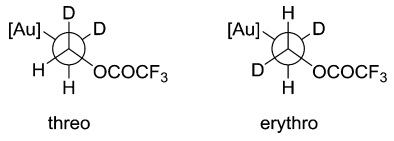

The expected different vicinal $^3J_{HH}$ coupling constants between the two methylene H atoms for the *threo* and *erythro* stereoisomers should give insight into whether there is an external or internal attack on ethylene. Bercaw and co-workers reported that $^3J_{HH}$ for the *threo* and *erythro* isomers of the Pt(IV) complex $[Pt(CHDCHDOH)Cl_5]^{2-}$ are 6 and 8 Hz, respectively.[66] The observed spectra (Supporting Information) exhibit two doublets as expected, with observed vicinal $^3J_{HH}$ coupling constants of approximately 6 Hz (6.1 and 5.7 Hz in TFA-*d* and dichloromethane-*d*$_2$, respectively), corresponding to the *threo* configuration. Formation of the *threo* product (Scheme 7) therefore strongly suggests that the product arises from external nucleophilic attack by $^-$OAc^F anion on coordinated ethylene. The product from the reaction was

Scheme 7. Reaction of 1 with *cis*-1,2-Dideuterioethylene Forms *threo*-2-*d*$_2$ by External Nucleophilic Attack

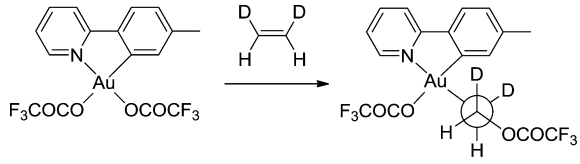

monitored over time, and no interconversion from the *threo* diastereomer to the *erythro* diastereomer could be observed in dichloromethane-*d*$_2$ over the course of several days. Also, no interconversion was observed in TFA-*d* after 1 day, but the onset of slow decomposition of **2-*d*$_2$** in TFA-*d* precluded monitoring of the reaction for a longer time.

DFT Calculations on the Reaction Mechanism. A computational study of the formal ethylene insertion into the Au−OAc^F bond in **1** was performed using DFT (PBE0-D3, see the Computational Details) calculations to support our experimental findings, guide experiments, and provide a deeper insight into the mechanism. As discussed in the presentation of the experimental results (vide supra), two fundamentally different mechanisms can be envisioned for this reaction: direct insertion of ethylene into the Au−OAc^F bond, or substitution of one OAc^F ligand by ethylene followed by nucleophilic addition of $^-$OAc^F. All attempts to find a transition state (TS) for the direct insertion of ethylene into the Au−O bonds were unsuccessful, and hence the initial substitution of one $^-$OAc^F anion by ethylene was explored (Scheme 8). This substitution process can be either dissociative or associative. The dissociation of the OAc^F ligand *trans* to N yields the 3-coordinate intermediate **4**, while dissociation *trans* to C leads to **4**$_C$. The free energies of the two intermediates are 30.6 and 16.3 kcal/mol, respectively, above **1**. The higher *trans* effect of C compared to N is in agreement with the lower energy of **4**$_C$. It is also found that **4**$_C$ is close in energy to the alternative isomer **5** with a κ^2-OAc^F ligand (17.2 kcal/mol; Au−O distances of 2.08 and 2.39 Å for the O atoms *trans* to N and *trans* to C, respectively). The computed free energy of **4**$_C$ compared to reactants suggests that dissociation of the OAc^F ligand *trans* to C should be feasible at room temperature. This conclusion is in agreement with the experimentally observed (^{19}F NMR) rapid equilibrium dissociation of the OAc^F ligand *trans* to C in polar solvents. In contrast, the high energy of **4** (30.6 kcal/mol) makes the involvement of this species highly unlikely. Interestingly, this high-energy species has the vacant coordination site in the appropriate position for the observed chemistry but is unlikely to be a kinetically competent intermediate under the reaction conditions.

Coordination of ethylene to **4** and **4**$_C$ yields **6** and **6**$_C$, which have associated free energies of 9.2 and 12.1 kcal/mol, respectively. The lower energy of **6** demonstrates a thermodynamic preference for the coordination of ethylene *trans* to N. The difference between the two is readily understood in terms of *trans* effects; the chelate C and ethylene are both high *trans* effect ligands and therefore prefer a mutual *cis*, rather than *trans*, relationship.

Since the formation of intermediate **6** (which has the ethylene in the appropriate position to give the observed product) by a dissociative pathway seems prohibited due to the high energy of **4**, the associative substitution of OAc^F *trans* to N was explored. To our satisfaction, such a transition state could be located (**TS1-6**, Scheme 8) with an energy of 21.8 kcal/mol,

dx.doi.org/10.1021/ja504554u | J. Am. Chem. Soc. 2014, 136, 10104−10115

Scheme 8. Ethylene Addition in 1 by Associative and Dissociative Substitution of OAc^F *Trans* to C and N[a]

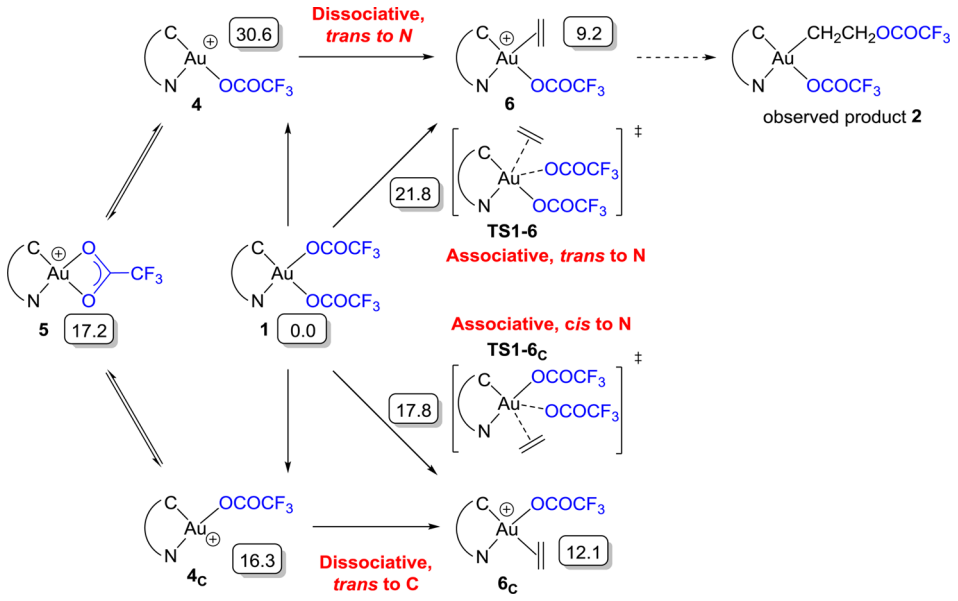

[a]Free energies are in kcal/mol in TFE. The energies of $^-OAc^F$ and ethylene have been included in the calculations where needed to maintain mass balance.

which is reasonable for a reaction that takes place at room temperature. Associative substitution *trans* to C is also possible and has an energy slightly higher than $\mathbf{4_C}$ ($\mathbf{TS1\text{-}6_C}$ = 17.8 kcal/mol). Thus, three energetically accessible pathways have been located that allow ethylene to coordinate at the Au center: *trans* to C by associative or dissociative pathways, and *trans* to N by an associative pathway. Since **6** and **6c** are accessible, nucleophilic addition of $^-OAc^F$ was considered from both intermediates.

Starting from the more thermally stable intermediate **6**, intermolecular and intramolecular mechanisms for the addition of OAc^F to the coordinated ethylene to form the observed product **2** were considered (Scheme 9). External (intermolecular) nucleophilic addition of the dissociated $^-OAc^F$ anion was found to occur with a low barrier through transition state **TS6-2** with a free energy of 13.8 kcal/mol, indicating a fast process. This addition leads directly to the experimentally observed product **2**, which is 6.9 kcal/mol lower in energy than the reactants (**1** and ethylene).

In contrast to the intermolecular mechanism, the calculations suggest that several steps are required in the alternative intramolecular addition pathway. It was not possible to locate a transition state that allows the direct, intramolecular nucleophilic attack by OAc^F on coordinated ethylene in the square planar complex when the ethylene C═C bond axis is oriented perpendicular to the coordination plane. Instead, the calculations suggest that before the nucleophilic attack by coordinated OAc^F can occur, the C═C bond axis must rotate from its preferred perpendicular orientation to a parallel (in-plane) orientation as depicted in **7** (Scheme 9). Subsequently, the intramolecular nucleophilic addition by the two oxygen atoms of coordinated OAc^F can take place through the two transition states **TS7-8** and **TS7-9** depicted in Scheme 9, leading to the six- and four-membered-ring intermediates **8** and **9**, located 1.4 and 14.5 kcal/mol above the reactants, respectively. Substitution of the κ(O) bonds of **8** and **9** by the external $^-OAc^F$ anion would finally yield the product **2**.

Scheme 9. Inter- and Intramolecular Nucleophilic Addition of OAc^F to 6[a]

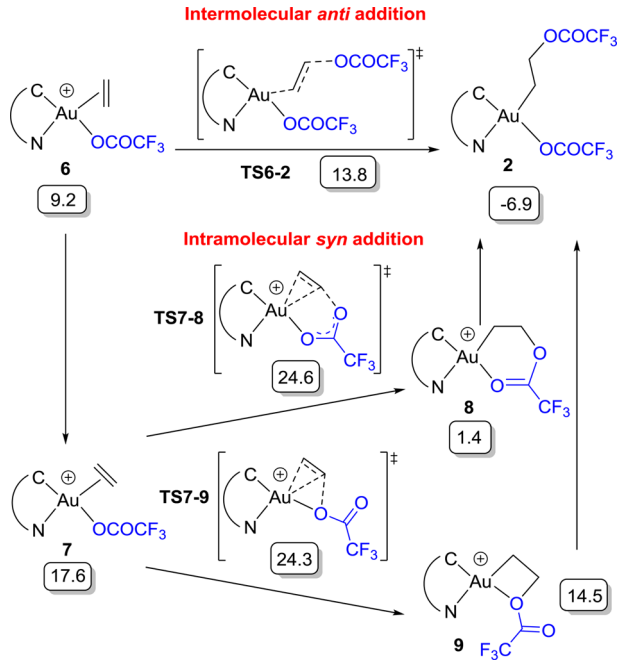

[a]Free energies in kcal/mol in TFE. The energy of $^-OAc^F$ has been included in the calculations where needed to maintain mass balance.

Although the energy barriers for the two intramolecular addition pathways from **7** (7.0 and 6.7 kcal/mol, respectively) are comparable to the energy barrier for the intermolecular addition from **6** (4.6 kcal/mol), the added energy cost (8.4 kcal/mol) incurred by changing the coordination mode of ethylene from perpendicular to parallel renders the intramolecular process kinetically much less favorable than the intermolecular one. These results are in complete agreement with the experimental results of the reaction between **1** and *cis*-

dx.doi.org/10.1021/ja504554u | J. Am. Chem. Soc. 2014, 136, 10104−10115

Scheme 10. Free Energy Profile (in kcal/mol) for the Formation of 2 (Right) and 2_C (Left)[a]

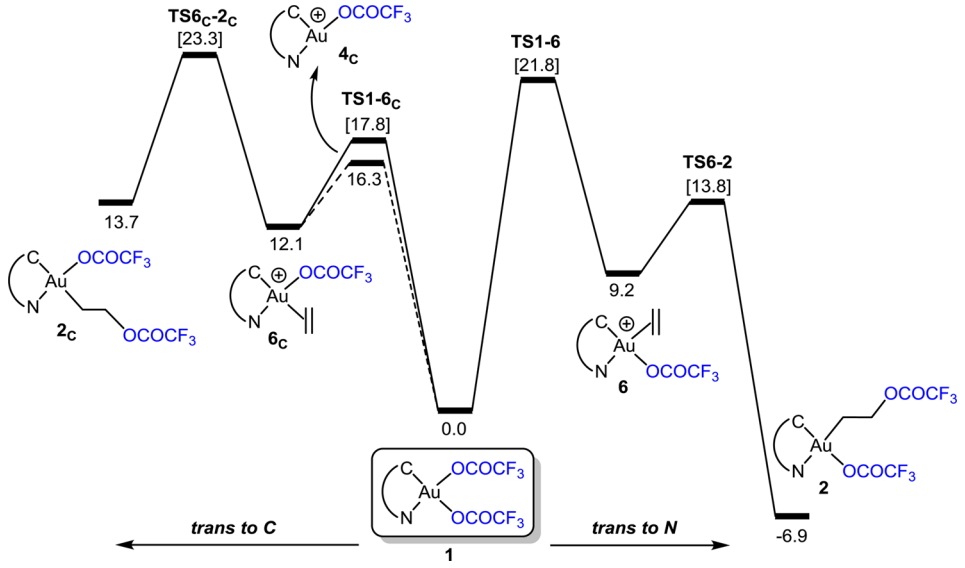

[a]The energies of all minima and transition states [in brackets] are computed in TFE. The energies of ethylene and $^{-}OAc^{F}$ have been included in the calculations to maintain mass balance.

1,2-dideuterioethylene (vide supra), which clearly demonstrated the intermolecular and *anti* addition of $^{-}OAc^{F}$. Interestingly, however, the computational results suggest that should a system exist in which a coplanar orientation of the olefin C═C bond axis and the nucleophile is preferred, then an intramolecular addition might be the favored pathway.

All the mechanistic alternatives computed for the nucleophilic addition of $^{-}OAc^{F}$ to **6** have also been considered starting from $\mathbf{6_C}$ (see that Supporting Information). All intermediates and transition states arising from $\mathbf{6_C}$ have substantially higher energies than the analogous species originating from **6**. For instance, the intermolecular addition of $^{-}OAc^{F}$ to $\mathbf{6_C}$ ($\mathbf{TS6_C\text{-}2_C}$), which represents the lowest-energy pathway from $\mathbf{6_C}$, has a global free energy barrier of 23.3 kcal/mol and the final product $\mathbf{2_C}$ is 13.7 kcal/mol above the reactants (Scheme 10). The endergonic nature of the formal insertion of ethylene into the Au−O bond *trans* to C is in stark contrast to the exergonic insertion *trans* to N and is in excellent agreement with the selective formation of product **2**.

In addition to the nucleophilic attack of $^{-}OAc^{F}$ on **6**, the nucleophilic addition of TFE to this intermediate was also considered since reaction of **1** with ethylene in TFE yields **3** instead of **2** (vide supra). Taking into account the large energy difference between the inter- and intramolecular addition of $^{-}OAc^{F}$ (Scheme 9), the intramolecular alternative was not considered with TFE. The intermolecular addition of TFE to **6** to form **3** and $HOAc^{F}$ can evolve through the protonated intermediate $[Au(tpy)(OAc^{F})(CH_2CH_2OHCH_2CF_3)]^{+}$ ($\mathbf{3H^{+}}$) or directly by assisted deprotonation of the alcohol by the $^{-}OAc^{F}$ anion ($\mathbf{TS6-3}$, Scheme 11). The latter pathway is the lowest in energy with an energy barrier of 8.3 kcal/mol and is exergonic by 12.1 kcal/mol. A comparison of these energies with the ones obtained for **2** ($\Delta\Delta G^{\ddagger}$ = 4.6 and $\Delta\Delta G^{\circ}$ = −16.1 kcal/mol), as shown in Scheme 11, suggest a kinetic and thermodynamic preference for the nucleophilic addition of $^{-}OAc^{F}$ over TFE. The thermodynamic preference for **2** calculated in TFE ($\Delta\Delta G^{\circ}$ = 4.0 kcal/mol) is also observed in dichloromethane ($\Delta\Delta G^{\circ}$ = 5.2 kcal/mol). This preference is in

Scheme 11. Free Energy Profile (in kcal/mol) for the Insertion of Ethylene to 1 (Black), Addition of TFE to 6 (Red), and Exchange of Ethylene of 6 (Green)[a]

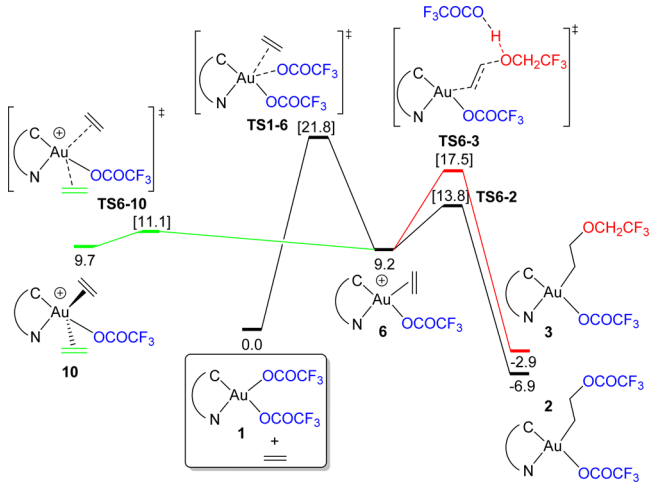

[a]The energies of all minima and transition states [in brackets] are computed in TFE. The energies of ethylene, $^{-}OAc^{F}$, and TFE have been included in the calculations where needed to maintain mass balance.

agreement with the experimental ΔG° = 1.1 kcal/mol in favor of **2**, and with the observation that **3** is not formed in dichloromethane when **1** is reacted with ethylene in the presence of 1.2 equiv of TFE. Importantly, the continuum SMD model used for solvation does not include explicit hydrogen bonds between dissolved species and the solvent.

The rate-determining step for the overall functionalization of ethylene is now, according to the calculations, the associative substitution of OAc^{F} *trans* to N by ethylene. As found experimentally and described earlier, the formation of **2** is much faster in TFA (ca. 5 min) and TFE (ca. 30 min) than in dichloromethane (ca. 1 day). A comparison of the energy profiles obtained in TFE (Scheme 11) and dichloromethane

dx.doi.org/10.1021/ja504554u | J. Am. Chem. Soc. 2014, 136, 10104−10115

(Scheme S2, Supporting Information) reveals that the higher free energy obtained for **TS1-6** in dichloromethane (25.1 kcal/mol) compared to the one in TFE (21.8 kcal/mol) accounts for the higher reaction rate observed in TFE. This is reasonable due to the incipient charge separation associated with **TS1-6**, which can be better stabilized by the more polar solvent TFE (ε 26.74[67]). However, the similar polarities of TFA and dichloromethane (ε 8.42 and 8.93, respectively[67]) suggest that this parameter is not enough to explain the reaction rate in TFA. Therefore, we propose that the ability of TFA to assist the departure of the $^{-}$OAc^{F} anion by protonation could be the reason for the faster formation of **2** in TFA. The magnitudes of the computed energies of **TS6-2** and **TS6-3** and the corresponding products **2** and **3** are consistent with the occurrence of thermal equilibration of **2** and **3** at ambient temperature (Scheme 11). Hence, considering equilibration to occur through intermediate **6**, the energy barrier that must be passed at **TS6-3** to form **2** from **3** is 20.4 kcal/mol, while the reverse process has an energy barrier of 24.4 kcal/mol defined from **2**. These free energy barriers are probably overestimated because they are computed using a 1 atm ideal gas standard state at 298.15 K and do not take into account the concentration effect of using TFE vs TFA (the source of the $^{-}$OAc^{F} anion) as the solvents. Indeed, just by applying the 1 M standard state for the free energy calculations, the energies of **2**, **3**, and **TS6-2** are reduced by 1.9 kcal/mol, and the energy of **TS6−3** is reduced by 3.8 kcal/mol (see Scheme S3, Supporting Information).

Finally, the experimentally observed exchange of ethylene for ethylene-d_4 in **2** (Scheme 4) has been addressed computationally. The fact that the ethylene has been demonstrated to be reversibly attacked by the nucleophiles suggests that intermediate **6** may be involved in the exchange process. One obvious pathway may be considered to be the regeneration of **1**, i.e., the reverse of the initial ethylene coordination that furnishes **6** from **1** via **TS1-6**. Starting from **2**, the energy barrier (**TS1-6**) for this process is as high as 28.7 kcal/mol. Alternatively, ethylene exchange might occur through an associative pathway via intermediate **10** (Scheme 11, green line), in which two ethylene units are simultaneously bonded to Au. Our recently reported,[42] structurally characterized complex $Me_2Au(cod)^{+}$ serves to demonstrate the viability of a bis(alkene) Au(III) species. The energy of the transition state to form this pentacoordinated intermediate (**TS6-10**) is 10.7 kcal/mol lower than **TS1-6** and 2.7 kcal/mol lower than **TS6-2**. Therefore, associative ethylene exchange through **10** appears to be the preferred process with an associated energy barrier of 18.0 kcal/mol starting from **2**. This is consistent with the observation of this exchange process at ambient temperature. Furthermore, this implies that the ethylene/ethylene-d_4 exchange does not occur by the regeneration of **1**, which agrees with the difficulties in regenerating **1** from **2** (as heating, with accompanying induced sample decomposition, is needed to observe **1**).

CONCLUSIONS

This study has provided a comprehensive, internally consistent and detailed view of a stoichiometric functionalization of ethylene at an Au(III) center. The mechanism of the formal ethylene insertion that is consistent with the accumulated experimental and computational data comprises a rate-limiting, strongly solvent-dependent, associative substitution[68−71] of the OAc^{F} ligand *trans* to N with ethylene, followed by intermolecular (*anti*) attack of the dissociated ligand at the coordinated ethylene to yield **2**, as verified by experiment using *cis*-1,2-dideuterioethylene as a stereochemical probe. Additionally, the poorer nucleophile TFE, when used as a solvent, can intermolecularly attack ethylene to provide **3**. The nucleophilic attack at ethylene has been shown to be reversible; such behavior has been previously observed at Au(I)[57] but to our knowledge not at Au(III). The preference for an intermolecular nucleophilic attack over an intramolecular one is a consequence of the energy required to reorient ethylene from a preferred coordination perpendicular to the Au(III) square plane to a coordination parallel to the square plane. Ethylene exchange takes place via an associative mechanism.

Complex **1** with the chelating tpy ligand provides two potential reaction sites, *trans* to N and *trans* to C, that will be kinetically nonequivalent because of their different *trans* effects. The experimentally and computationally consistent reaction mechanism illustrates the influence of this guiding principle. The first step of the reaction, ethylene coordination, is kinetically preferred *trans* to C (the ligand with the highest *trans* effect). The second step of the reaction, addition of a nucleophile to the ethylene, provides a product **2** or **3** that is thermodynamically favored to be *trans* to N. Here, the dichotomy is overcome through an associative substitution of ethylene *trans* to N, via **TS1-6** to give **6**. While this process has a higher energy barrier than that for ethylene substitution *trans* to C to give $\mathbf{6_C}$, as illustrated in Scheme 10, the thermodynamic preference of **2** over $\mathbf{2_C}$ results in the exclusive formation of the preferred *trans* to N products **2** and **3**.

Our initial efforts to encourage a catalytic reaction have not met with success. The Au(III)−alkyl σ bond can be remarkably resistant toward acids, an aspect that must be further addressed if catalysis is to be achieved. In this reaction, protic solvents (TFA, TFE) accelerate the reaction (as compared to dichloromethane), most likely through stabilization of the dissociated $^{-}$OAc^{F} anion, but they do not otherwise show any reactivity with either **1**, **2**, or **3**. The use of protic solvents in the functionalization of olefins by Au(I) has been shown to be essential in some catalytic processes because it promotes concerted addition of the nucleophile and protodeauration.[72] For a hypothetical Au(III) catalytic process, protodeauration could again be preferred *trans* to C,[73] suggesting that this *trans* to C/*trans* to N dichotomy must again be overcome to complete a catalytic cycle that does not require additional stoichiometric reagents to regenerate a Au(III) species.

Investigations are ongoing in our laboratory that concern the insertion of other alkenes and alkynes, the use of other nucleophiles than TFA and TFE, and to utilize the insight gained in the design of catalytic processes.

EXPERIMENTAL AND COMPUTATIONAL SECTION

General Experimental Methods. TFA, TFE, and NMR solvents were used as received. The Au(III) complexes are not air sensitive, so inert atmosphere was not utilized. The microwave oven used was of the type Milestone MicroSYNTH with a rotor of the type SK-10. NMR spectra were recorded on a Bruker Avance AV600 operating at 600 MHz (^{1}H), DRX500 operating at 500 MHz (^{1}H), AVII400 operating at 400 MHz (^{1}H), and DPX200 operating at 200 MHz (^{1}H). ^{1}H and ^{13}C spectra have been referenced relative to the residual solvent signals. ^{19}F spectra has been referenced to C_6F_6 (−164.9 ppm with respect to $CFCl_3$ at 0.0 ppm) as an internal standard. 1,2-Dichloroethane (chemicals shifts in CD_2Cl_2: 3.76 ppm; TFA-*d*; 3.58 ppm, TFE-d_3; 3.70 ppm) was used as an internal standard in several of the ^{1}H NMR experiments. All NMR spectra are recorded at ambient

dx.doi.org/10.1021/ja504554u | J. Am. Chem. Soc. 2014, 136, 10104−10115

temperature unless otherwise noted. ^{1}H NMR assignments were made on the basis of COSY and NOESY experiments and refer to the numbering schemes shown below. Mass spectrometry was performed with Waters ProSpec (EI) and Q-TOF-2 (ESI) instruments. Elemental analyses were performed by Mikroanalytisches Laboratorium Kolbe, Mülheim an der Ruhr, Germany. Details of the crystallographic methods and structure determinations are given in the Supporting Information.

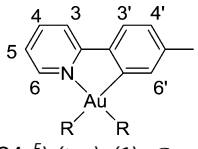

*Preparation of Au(OAc^F)$_2$(tpy) (**1**).* Compound **1** was prepared according to the recently reported method,[46] except that $Au(OH)_3$ was used instead of $Au(OAc)_3$ under otherwise identical conditions. The only difference was that filtration instead of decantation was used to remove the unreacted gold precursor, which did not settle to the bottom of the microwave vessel in this case. Starting from $Au(OH)_3$ the yield was however somewhat lower (72% vs 94%). See the Supporting Information for NMR data in dichloromethane-d_2 (previously reported) and other solvents.

*Preparation of Au(OAc^F)(CH$_2$CH$_2$OAc^F)(tpy) (**2**).* Ethylene gas was bubbled through a solution of $Au(OAc^F)_2$(tpy) (**1**) (0.202 g, 0.341 mmol) in TFA in a septum-capped round-bottom flask equipped with a vent needle at ambient temperature for 2 h. The solution changed from a light yellow color to colorless within a few minutes. The solvent was removed under reduced pressure to yield a light gray powder which was dissolved in dichloromethane and filtered to give a light yellow solution. The solution was concentrated under reduced pressure and layered with pentane. Crystallization gave large yellow crystals (0.161 g, 76%). ^{1}H NMR (600 MHz, CD_2Cl_2): δ 8.38 (ddd, 6-C*H*, J = 5.5, 1.7, 0.8 Hz, 1H), 8.04 (ddd, 4-C*H*, J = 7.6, 7.6, 1.7 Hz, 1H), 7.93 (d, 3-C*H*, J = 8.2 Hz, 1H), 7.64 (d, 3′-C*H*, J = 7.9 Hz, 1H), 7.48 (ddd, 5-C*H*, J = 7.2, 5.6, 1.3 Hz, 1H), 7.36 (s, 6′-C*H*, 1H), 7.22 (ddd, 4′-C*H*, J = 7.8, 1.6, 0.8 Hz, 1H), 4.83−4.69 (m, CH_2O, 2H), 2.45 (s, ArCH_3, 3H), 2.43−2.36 (m, AuCH_2, 2H). ^{13}C NMR (151 MHz, CD_2Cl_2): δ 161.6 (q, CO, J = 37.1 Hz), 161.2, 158.0 (q, CO, J = 41.8 Hz), 146.5, 143.5, 142.4, 140.9, 136.5, 132.2, 129.7, 126.1, 124.6, 120.6, 118.3 (q, CF_3, J = 290.0 Hz), 115.1 (q, CF_3, J = 285.9 Hz), 68.9, 26.9, 22.1. ^{19}F NMR (377 MHz, CD_2Cl_2): δ −77.0 (s, $CF_{3\ (cis\ to\ N)}$, 3F), −77.8 (s, $CF_{3\ (trans\ to\ N)}$, 3F). MS (EI in CH_3CN): m/z = 505.9 (40, [M − $COOCF_3$]$^+$), 477.9 (92, [M − $CH_2CH_2OCOCF_3$]$^+$), 169.0 (100). MS-HR (CH_3CN): m/z = 506.064479 (calcd for $C_{16}H_{14}AuF_3NO_2$ 506.064224 (−0.5 ppm)), 478.032024 (calcd for $C_{14}H_{10}AuF_3NO_2$ 478.032923 (1.9 ppm)). Anal. Calcd for $C_{18}H_{14}AuF_6NO_4$: C, 34.91; H, 2.28; N, 2.26. Found: C, 34.53; H, 2.26; N, 2.24.

*Preparation of Au(OAc^F)(CH$_2$CH$_2$OCH$_2$CF$_3$)(tpy) (**3**).* Ethylene gas was bubbled through a solution of $Au(OAc^F)_2$(tpy) (**1**) (0.202 g, 0.341 mmol) in TFE in a septum-capped round-bottom flask equipped with a vent needle at ambient temperature for 2 h. The solution changed from a light yellow color to colorless over time. The solvent was removed under reduced pressure to yield a light gray powder which was dissolved in dichloromethane and filtered to give a light yellow solution. The solution was concentrated under reduced pressure and layered with pentane. Crystallization gave the product as white needles (0.140 g, 68%). Due to the equilibrium between **2** and **3** it was not possible to isolate pure **3**, as there was always some **2** present (<5%). ^{1}H NMR (500 MHz, CD_2Cl_2): δ 8.32 (ddd, 6-C*H*, J = 5.5, 1.7, 0.8 Hz, 1H), 8.00 (ddd, 4-C*H*, J = 8.2, 7.5, 1.6, Hz, 1H), 7.90 (d, 3-C*H*, J = 8.2 Hz, 1H), 7.60 (d, 3′-C*H*, J = 7.9 Hz, 1H), 7.44 (ddd, 5-C*H*, J = 7.5, 5.5, 1.3 Hz, 1H), 7.24 (s, 6′-C*H*, 1H), 7.18 (ddd, 4′-C*H*, J = 8.0, 1.7, 0.9 Hz, 1H), 3.95−3.92 (m, CH_2O, 2H), 3.90 (q, CH_2CF$_3$, J = 8.8 Hz, 2H), 2.40 (s, ArCH_3, 3H), 2.37−2.31 (m, AuCH_2, 2H). ^{13}C NMR (151 MHz, CD_2Cl_2): δ 161.5 (q, CO, J = 36.8 Hz), 160.9, 146.4, 143.0, 142.1, 141.0, 136.5, 132.1, 129.5, 126.0, 124.9 (q, CF_3, J = 279.6 Hz), 124.5, 120.5, 118.4 (q, CF_3, J = 290.0 Hz), 72.3, 68.3 (q, CH_2, J = 33.6 Hz), 30.5, 22.1. ^{19}F NMR (377 MHz, CD_2Cl_2): δ −76.9 (s, $CF_{3\ (trans\ to\ N)}$, 3F), −77.0 (s, $CF_{3\ (cis\ to\ N)}$, 3F). MS (EI in CH_3CN): m/z = 491.9 (40, [M − $COOCF_3$]$^+$), 477.9 (54, [M − $CH_2CH_2OCH_2CF_3$]$^+$), 196.0 (100). MS-HR (CH_3CN): m/z = 492.083643 (calcd for $C_{16}H_{16}AuF_3NO$ 492.084959 (2.7 ppm)), 478.032606 (calcd for $C_{14}H_{10}AuF_3NO_2$ 478.032923 (0.7 ppm)). No elemental analysis was performed for this compound because samples always contained some **2** (see the Results and Discussion).

General Method for NMR Experiments. A J-Young NMR tube was loaded with the pertinent Au(III) complex (ca. 5 mg) and internal standard (CH_2ClCH_2Cl, 1.0 μL), whereupon the solvent (TFA-d, TFE-d_3, or CD_2Cl_2, ca. 0.5 mL) was added. A reference spectrum was acquired. Ethylene was bubbled through the solution for 30−60 s. In TFA-d and TFE-d_3 this caused the yellow solution to turn colorless. A new ^{1}H NMR spectrum was acquired within 5−10 min.

High-Pressure NMR Experiments. The high-pressure NMR experiments were conducted at École Polytechnique Fédérale de Lausanne (EPFL) using sapphire NMR tubes (for 10 mm probes) that can endure pressures up to 100 bar.[74,75]

COMPUTATIONAL DETAILS

The calculations were carried out at the DFT level with Gaussian 09.[76] PBE0[77] was the functional selected as it has been previously shown to give the best results in recent studies on Au(III) alkene complexes.[42,78] C and H were described with the all-electron triple-ζ 6-311+G** basis set,[79,80] whereas Au was described with the new Stuttgart−Köln basis set including a small-core quasi-relativistic pseudopotential.[81] Geometries were fully optimized without any constraint. Vibrational frequencies were computed analytically to verify that the stationary points found were energy minima or transition states. Each transition state was relaxed toward reactant and product by using the vibrational data to confirm its nature. All optimizations were carried out in solvent (2,2,2-trifluoroethanol) using the SMD solvation model.[82] Grimme dispersion corrections (D3)[83] were included in the final energy by performing single point calculations on the optimized structures. Gibbs energies were obtained for T = 298.15 K and p = 1 atm within the approximation of harmonic frequencies. The effect of using 1 M standard state (T = 298.15 K and p = 24.465 atm) was evaluated in some minima and transition states (see Scheme S3 in the Supporting Information), and in all cases, the energy was reduced by 1.9 kcal/mol when the molecularity changes from two to one, and by 3.8 kcal/mol (as in **TS1-6**) when going from three to one (as in **TS6-3**). Optimized energies and geometries of all stationary points reported in the text are given in the Supporting Information.

ASSOCIATED CONTENT

Supporting Information

Characterization, crystallographic, and computational data. This material is available free of charge via the Internet at http://pubs.acs.org.

AUTHOR INFORMATION

Corresponding Authors

ainara.nova@kjemi.uio.no
mats.tilset@kjemi.uio.no

Notes

The authors declare no competing financial interest.

ACKNOWLEDGMENTS

This work has been supported by the Research Council of Norway through a Centre of Excellence Grant (Grant No. 179568/V30) and the Norwegian Supercomputing Program (NOTUR) through a grant of computer time (Grant No. NN4654K). Prof. G. Laurenzy is greatly acknowledged for helping with the high-pressure NMR experiments, M. S. Holmsen for taking part in the high-pressure NMR experiments, and O. Eisenstein and D. Balcells for fruitful discussions.

E.L. thanks COST for support through COST Action No. CM1205.

REFERENCES

(1) *Modern Gold Catalyzed Synthesis*; Hashmi, A. S. K., Toste, F. D., Eds.; Wiley-VCH Verlag: Weinheim, 2012.
(2) *Gold Catalysis: An Homogeneous Approach*; Toste, F. D., Michelet, V., Eds.; Imperial College Press: London, 2012.
(3) Hashmi, A. S. K. *Chem. Rev.* **2007**, *107*, 3180−3211.
(4) Li, Z.; Brouwer, C.; He, C. *Chem. Rev.* **2008**, *108*, 3239−3265.
(5) Arcadi, A. *Chem. Rev.* **2008**, *108*, 3266−3325.
(6) Jiménez-Núñez, E.; Echavarren, A. M. *Chem. Rev.* **2008**, *108*, 3326−3350.
(7) Fürstner, A. *Chem. Soc. Rev.* **2009**, *38*, 3208−3221.
(8) Shapiro, N. D.; Toste, F. D. *Synlett* **2010**, 675−691.
(9) Rudolph, M.; Hashmi, A. S. K. *Chem. Commun.* **2011**, *47*, 6536−6544.
(10) Corma, A.; Leyva-Pérez, A.; Sabater, M. J. *Chem. Rev.* **2011**, *111*, 1657−1712.
(11) Bandini, M. *Chem. Soc. Rev.* **2011**, *40*, 1358−1367.
(12) Rudolph, M.; Hashmi, A. S. K. *Chem. Soc. Rev.* **2012**, *41*, 2448−2462.
(13) Leyva-Pérez, A.; Corma, A. *Angew. Chem., Int. Ed.* **2012**, *51*, 614−635.
(14) Schmidbaur, H.; Schier, A. *Arab. J. Sci. Eng.* **2012**, *37*, 1187−1225.
(15) Wegner, H. A. *Chimia* **2009**, *63*, 44−48.
(16) Wegner, H. A.; Auzias, M. *Angew. Chem., Int. Ed.* **2011**, *50*, 8236−8247.
(17) Hopkinson, M. N.; Gee, A. D.; Gouverneur, V. *Chem.—Eur. J.* **2011**, *17*, 8248−8262.
(18) de Haro, T.; Nevado, C. *Synthesis* **2011**, 2530−2539.
(19) Ball, L. T.; Lloyd-Jones, G. C.; Russell, C. A. *J. Am. Chem. Soc.* **2014**, *136*, 254−264.
(20) Soriano, E.; Marco-Contelles, J. *Top. Curr. Chem.* **2011**, *302*, 1−29.
(21) Tkatchouk, E.; Mankad, N. P.; Benitez, D.; Goddard, W. A., III; Toste, F. D. *J. Am. Chem. Soc.* **2011**, *133*, 14293−14300.
(22) Lv, H.; Zhan, J.-H.; Cai, Y.-B.; Yu, Y.; Wang, B.; Zhang, J.-L. *J. Am. Chem. Soc.* **2012**, *133*, 16216−16227.
(23) Basak, A.; Chakrabarty, K.; Ghosh, A.; Das, G. K. *J. Org. Chem.* **2013**, *78*, 9715−9724.
(24) Comas-Vives, A.; Ujaque, G. *J. Am. Chem. Soc.* **2013**, *135*, 1295−1305.
(25) Wang, Y.; McGonigal, P. R.; Herlé, B.; Besora, M.; Echavarren, A. M. *J. Am. Chem. Soc.* **2014**, *136*, 801−809.
(26) Hashmi, A. S. K. *Angew. Chem., Int. Ed.* **2012**, *51*, 12935−12936.
(27) Roşca, D.-A.; Smith, D. A.; Hughes, D. L.; Bochmann, M. *Angew. Chem., Int. Ed.* **2012**, *51*, 10643−10646.
(28) Schmidbaur, H.; Schier, A. *Organometallics* **2010**, *29*, 2−23.
(29) Brooner, R. E. M.; Widenhoefer, R. A. *Angew. Chem., Int. Ed.* **2013**, *52*, 11714−11724.
(30) Guenther, J.; Mallet-Ladeira, S.; Estevez, L.; Miqueu, K.; Amgoune, A.; Bourissou, D. *J. Am. Chem. Soc.* **2014**, *136*, 1778−1781.
(31) Joost, M.; Gualco, P.; Coppel, Y.; Miqueu, K.; Kefalidis, C. E.; Maron, L.; Amgoune, A.; Bourissou, D. *Angew. Chem., Int. Ed.* **2014**, *53*, 747−751.
(32) Mankad, N. P.; Toste, F. D. *Chem. Sci.* **2012**, *3*, 72−76.
(33) Ghidiu, M. J.; Pistner, A. J.; Yap, G. P. A.; Lutterman, D. A.; Rosenthal, J. *Organometallics* **2013**, *32*, 5026−5029.
(34) Wolf, W. J.; Winston, M. S.; Toste, F. D. *Nat. Chem.* **2014**, *6*, 159−164.
(35) Dupuy, S.; Slawin, A. M. Z.; Nolan, S. P. *Chem.—Eur. J.* **2012**, *18*, 14923−14928.
(36) Chen, Y.; Chen, M.; Liu, Y. *Angew. Chem., Int. Ed.* **2012**, *51*, 6181−6186.
(37) delPozo, J.; Carrasco, D.; Pérez-Temprano, M. H.; García-Melchor, M.; Álvarez, R.; Casares, J. A.; Espinet, P. *Angew. Chem., Int. Ed.* **2013**, *52*, 2189−2193.
(38) Hashmi, A. S. K. *Angew. Chem., Int. Ed.* **2010**, *49*, 5232−5241.
(39) Liu, L.-P.; Hammond, G. B. *Chem. Soc. Rev.* **2012**, *41*, 3129−3139.
(40) Chiarucci, M.; Bandini, M. *Beilstein J. Org. Chem.* **2013**, *9*, 2586−614.
(41) Savjani, N.; Roşca, D.-A.; Schormann, M.; Bochmann, M. *Angew. Chem., Int. Ed.* **2013**, *52*, 874−877.
(42) Langseth, E.; Scheuermann, M. L.; Balcells, D.; Kaminsky, W.; Goldberg, K. I.; Eisenstein, O.; Heyn, R. H.; Tilset, M. *Angew. Chem., Int. Ed.* **2013**, *52*, 1660−1663.
(43) Keith, J. A.; Nielsen, R. J.; Oxgaard, J.; Goddard, W. A., III. *J. Am. Chem. Soc.* **2007**, *129*, 12342−12343.
(44) Keith, J. A.; Henry, P. M. *Angew. Chem., Int. Ed.* **2009**, *48*, 9038−9049.
(45) Rezsnyak, C. E.; Autschbach, J.; Atwood, J. D.; Moncho, S. *J. Coord. Chem.* **2013**, *66*, 1153−1165.
(46) Langseth, E.; Görbitz, C. H.; Heyn, R. H.; Tilset, M. *Organometallics* **2012**, *31*, 6567−6571.
(47) A comparison of the ^{19}F spectra are included in the Supporting Information.
(48) Mahon, M. F.; Whittlesey, M. K.; Wood, P. T. *Organometallics* **1999**, *18*, 4068−4074.
(49) Chaudhari, S. R.; Mogurampelly, S.; Suryaprakash, N. *J. Phys. Chem. B* **2013**, *117*, 1123−1129.
(50) Li, H.; Frieden, C. *Biochemistry* **2006**, *45*, 6272−6278.
(51) Buchanan, G. W.; Munteanu, E.; Dawson, B. A.; Hodgson, D. *Magn. Reson. Chem.* **2005**, *43*, 528−534.
(52) Battiste, J. L.; Jing, N.; Newmark, R. A. *J. Fluorine Chem.* **2004**, *125*, 1331−1337.
(53) Plaumann, M.; Bommerich, U.; Trantzschel, T.; Lego, D.; Dillenberger, S.; Sauer, G.; Bargon, J.; Buntkowsky, G.; Bernarding, J. *Chem.—Eur. J.* **2013**, *19*, 6334−6339.
(54) Battiste, J.; Newmark, R. A. *Prog. Nucl. Magn. Reson. Spectrosc.* **2006**, *48*, 1−23.
(55) Acetonitrile-d_3, 188 MHz, 25 °C, QNP-probe. Acquisition parameters: d_8 = 0.30 s, ns = 8, d_1 = 2.0s, aq(F2,F1) = 0.50 s, 0.06 s, sw = 10.85 ppm.
(56) High-pressure NMR experiments were conducted in sapphire tubes under the guidance of Prof. Gabor Laurenzy at École Polytechnique Fédérale de Lausanne (EPFL), Switzerland. Heating a solution of **1** in TFA at 50 °C under 60 atm of ethylene led to decomposition. No evidence for catalytic conversion of ethylene or signals that might be attributed to Au(III) ethylene complexes, was observed.
(57) LaLonde, R. L.; Brenzovich, W. E., Jr.; Benitez, D.; Tkatchouk, E.; Kelley, K.; Goddard, W. A., III; Toste, F. D. *Chem. Sci.* **2010**, *1*, 226−233.
(58) The errors in K_{eq} and $\Delta G°$ are ± one standard deviation of the mean.
(59) Krauter, C. M.; Hashmi, A. S. K.; Pernpointner, M. *ChemCatChem* **2010**, *2*, 1226−1230.
(60) Joost, M.; Gualco, P.; Mallet-Ladeira, S.; Amgoune, A.; Bourissou, D. *Angew. Chem., Int. Ed.* **2013**, *52*, 7160−7163.
(61) Hashmi, A. S. K.; Weyrauch, J. P.; Frey, W.; Bats, J. W. *Org. Lett.* **2004**, *6*, 4391−4394.
(62) Zhu, J.; Germain, A. R.; Porco, J. A., Jr. *Angew. Chem., Int. Ed.* **2004**, *43*, 1239−1243.
(63) Kovács, G.; Lledós, A.; Ujaque, G. *Angew. Chem., Int. Ed.* **2011**, *50*, 11147−11151.
(64) Johnson, M. W.; Shevick, S. L.; Toste, F. D.; Bergman, R. G. *Chem. Sci.* **2013**, *4*, 1023−1027.
(65) Bäckvall, J. E.; Åkermark, B.; Ljunggren, S. O. *J. Am. Chem. Soc.* **1979**, *101*, 2411−2416.
(66) Luinstra, G. A.; Wang, L.; Stahl, S. S.; Labinger, J. A.; Bercaw, J. E. *J. Organomet. Chem.* **1995**, *504*, 75−91.
(67) Permittivity (Dielectric Constant) of Liquids. In *CRC Handbook of Chemistry and Physics*, 94th ed. (Internet Version); Haynes, W. M., Ed.; CRC Press/Taylor and Francis: Boca Raton, FL, 2014.
(68) Cross, R. J. *Adv. Inorg. Chem.* **1989**, *34*, 219−292.

(69) Dos Santos, H. F.; Paschoal, D.; Burda, J. V. *J. Phys. Chem. A* **2012**, *116*, 11015−11024.
(70) Djeković, A.; Petrović, B.; Bugarčić, Ž. D.; Puchta, R.; van Eldik, R. *Dalton Trans.* **2012**, *41*, 3633−3641.
(71) Monlien, F. J.; Helm, L.; Abou-Hamdan, A.; Merbach, A. E. *Inorg. Chim. Acta* **2002**, *331*, 257−269.
(72) Kovács, G.; Lledós, A.; Ujaque, G. *Organometallics* **2010**, *29*, 3252−3260.
(73) Smith, D. A.; Roşca, D.-A.; Bochmann, M. *Organometallics* **2012**, *31*, 5998−6000.
(74) Roe, D. C. *J. Magn. Reson.* **1985**, *63*, 388−391.
(75) Cusanelli, A.; Frey, U.; Richens, D. T.; Merbach, A. E. *J. Am. Chem. Soc.* **1996**, *118*, 5265−5271.
(76) Frisch, M. J.; Trucks, G. W.; Schlegel, H. B.; Scuseria, G. E.; Robb, M. A.; Cheeseman, J. R.; Scalmani, G.; Barone, V.; Mennucci, B.; Petersson, G. A.; Nakatsuji, H.; Caricato, M.; Li, X.; Hratchian, H. P.; Izmaylov, A. F.; Bloino, J.; Zheng, G.; Sonnenberg, J. L.; Hada, M.; Ehara, M.; Toyota, K.; Fukuda, R.; Hasegawa, J.; Ishida, M.; Nakajima, T.; Honda, Y.; Kitao, O.; Nakai, H.; Vreven, T.; Montgomery, J. A., Jr.; Peralta, J. E.; Ogliaro, F.; Bearpark, M.; Heyd, J. J.; Brothers, E.; Kudin, K. N.; Staroverov, V. N.; Kobayashi, R.; Normand, J.; Raghavachari, K.; Rendell, A.; Burant, J. C.; Iyengar, S. S.; Tomasi, J.; Cossi, M.; Rega, N.; Millam, J. M.; Klene, M.; Knox, J. E.; Cross, J. B.; Bakken, V.; Adamo, C.; Jaramillo, J.; Gomperts, R.; Stratmann, R. E.; Yazyev, O.; Austin, A. J.; Cammi, R.; Pomelli, C.; Ochterski, J. W.; Martin, R. L.; Morokuma, K.; Zakrzewski, V. G.; Voth, G. A.; Salvador, P.; Dannenberg, J. J.; Dapprich, S.; Daniels, A. D.; Farkas, Ö.; Foresman, J. B.; Ortiz, J. V.; Cioslowski, J.; Fox, D. J. *Gaussian 09, Rev. B.01*; Gaussian Inc.: Wallingford, CT, 2009.
(77) Adamo, C.; Barone, V. *J. Chem. Phys.* **1999**, *110*, 6158−6170.
(78) Kang, R.; Chen, H.; Shaik, S.; Yao, J. *J. Chem. Theory Comput.* **2011**, *7*, 4002−4011.
(79) McLean, A. D.; Chandler, G. S. *J. Chem. Phys.* **1980**, *72*, 5639−5648.
(80) Krishnan, R.; Binkley, J. S.; Seeger, R.; Pople, J. A. *J. Chem. Phys.* **1980**, *72*, 650−654.
(81) Figgen, D.; Rauhut, G.; Dolg, M.; Stoll, H. *Chem. Phys.* **2005**, *311*, 227−244.
(82) Marenich, A. V.; Cramer, C. J.; Truhlar, D. G. *J. Phys. Chem. B* **2009**, *113*, 6378−6396.
(83) Grimme, S.; Antony, J.; Ehrlich, S.; Krieg, H. *J. Chem. Phys.* **2010**, *132*, 154104/1−154104/19.